



0017-9310(94)00263-0

Nucleate pool boiling of R-114 and R-114-oil mixtures from smooth and enhanced surfaces—I. Single tubes

S. B. MEMORY

Department of Mechanical Engineering, University of Miami, Coral Gables, FL 33124, U.S.A.

and

D. C. SUGIYAMA and P. J. MARTO

Department of Mechanical Engineering, Naval Postgraduate School, Monterey, CA 93943, U.S.A.

(Received 13 December 1993 and in final form 4 August 1994)

Abstract—Measurements of pool-boiling heat-transfer coefficients in pure R-114 and R-114-oil mixtures are reported for a smooth tube and eight enhanced tubes (five finned and three re-entrant cavity). Tests were carried out at atmospheric pressure while decreasing the heat flux. For pure refrigerant, the finned tubes typically provide enhancements of between 3 and 4, whilst the re-entrant cavity tubes provide enhancements of more than 10 at low heat fluxes, decreasing to around 4 at high heat fluxes. With addition of oil, performance of the finned tubes at first increases (with 3% oil) before dropping off. For the re-entrant cavity tubes, addition of oil causes a steady drop-off in performance, especially for the porous tube where heat transfer rates similar to that of the smooth tube were obtained.

INTRODUCTION

In recent years, considerable efforts have been spent in finding ways to design more compact evaporators for the process and refrigeration industries by using enhanced heat transfer surfaces. These surfaces can take a number of forms from simple low integral-fins (with varying fin profile) to more complicated re-entrant cavity type surfaces (structured and porous coated), as shown in Fig. 1.

Boiling mechanisms from smooth and enhanced surfaces for a single-component liquid are very complex. Leiner and Gorenflo [1] present a concise schematic of the mechanisms which affect heat transfer in nucleate pool boiling. For smooth tubes, Carey [2] provides an excellent summary of the attempts to model these mechanisms as well as those which affect bubble growth, departure size and departure frequency near a heated surface. Carey [2] and Stephan [3] summarize some of the correlations that are commonly used in nucleate pool boiling. Attempts to pre-

dict boiling behavior on enhanced surfaces have met with more limited success [4–8]. Further complexities are introduced with the addition of a second, less volatile component, such as refrigeration oil. Modeling of refrigerant-oil mixture behavior is presently limited to smooth tubes [9–11] and is highly empirical in nature. As discussed by Lloyd and Marto [12], in the absence of critical properties such as mass and thermal diffusion coefficients, modeling heat transfer performance of a refrigerant-oil mixture will remain difficult and chiller design will rely heavily on accurate experimental pool boiling data covering a wide variety of conditions and fluids.

Much data exists on pool boiling heat transfer from smooth and enhanced surfaces for a wide variety of refrigerants (for excellent detailed reviews on enhanced boiling heat transfer, the reader is referred to the books by Thome [13] and Webb [14]). For low integral-fin tubes with trapezoidal fin profiles (ranging from 19 to 40 fpi), typical enhancements[†] of up to 4 have been obtained [15–20]. Factors affecting enhancement include heat flux, system pressure, fin density and the fluid physical properties.[‡] When comparing data from different sources, care must be taken that one is consistent in the choice of tube surface area in the calculation of heat flux. If actual wetted area were used, reported enhancements would be significantly lower. Indeed, Sauer *et al.* [16] showed that

[†] Enhancement is defined as the heat-transfer coefficient for the enhanced tube divided by the heat-transfer coefficient for a smooth tube (with a diameter equal to the root diameter) under conditions of identical heat flux.

[‡] The enhancement is also significantly affected by the choice of tube diameter in the calculation of tube surface area.

NOMENCLATURE

d	outside tube diameter (root diameter or base of enhancement)	\bar{T}_w	average outside wall temperature
\dot{q}''	heat flux based on outside surface area (using d)	ΔT	wall superheat, ($\bar{T}_w - T_{sat}$)
T_{sat}	saturation temperature of pool	\bar{h}	average heat-transfer coefficient, $\dot{q}''/\Delta T$.

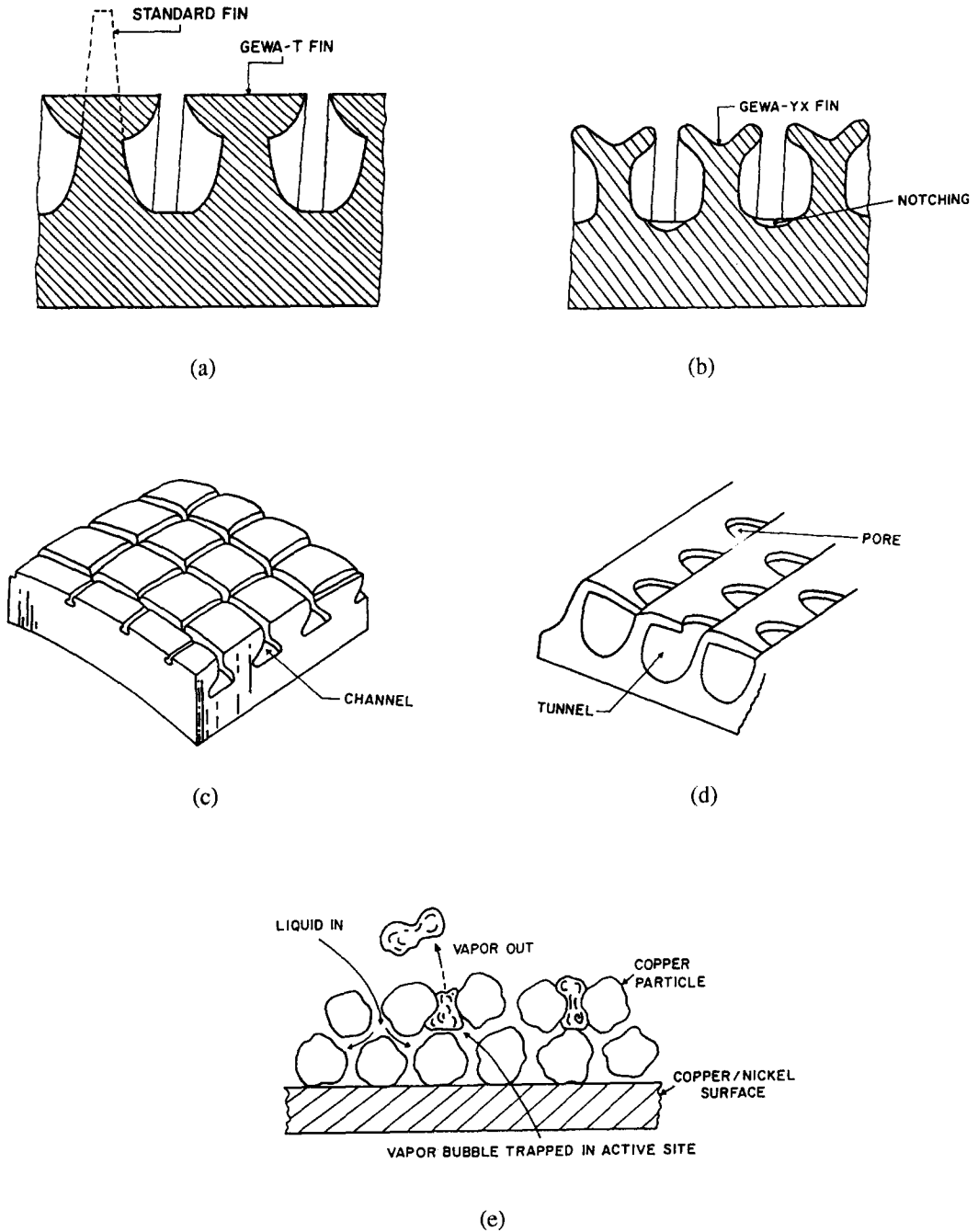


Fig. 1. Enhanced tubes tested. (a) Finned (GEWA-K and GEWA-T). (b) Finned (GEWA-YX). (c) Structured (TURBO-B). (d) Structured (THERMOEXCEL-HE). (e) Porous (HIGH FLUX).

for a 19 fpi tube at values of heat flux greater than 20 kW m^{-2} , using actual wetted area yielded lower heat transfer performance than a smooth tube with a diameter equal to the fin tip diameter.†

Many investigators have studied low integral-fin tubes with varying fin profiles [Fig. 1(a) and (b)] as a means of further enhancing heat-transfer [7, 18–25]. However, typical enhancements are only slightly better than with trapezoidal integral-fins. With these profiled fin tubes, the gap width has been found to have a stronger effect on thermal performance than fin density, with an optimum of around 0.25 mm for refrigerants [18, 21, 25]. Gorenflo *et al.* [20] further report that, for all types of low integral-fin tube, there is a sharp drop-off in enhancement with increase in system pressure and that, as the pressure approaches the critical value, all enhancement vanishes. Re-entrant cavity tubes come in two types: structured surface tubes and porous coated tubes. Although very different, both types of tube provide a high density of re-entrant cavities from which active stable nucleation sites can be maintained at a lower wall superheat: enhancements of more than 10 have been reported for pure refrigerants using both types [17, 19, 24, 26–33]. Pore size and gap width are critical parameters in enhancement and tube manufacturers are now ‘adjusting’ these to suit particular fluids and applications.

With a small amount of miscible oil added to a refrigerant (typically less than 3%), a number of investigators [16, 22, 26, 27, 32, 34] have reported small increases in the heat-transfer coefficient of up to 20% at high heat fluxes ($> 50 \text{ kW m}^{-2}$) for smooth and low integral-fin tubes when compared with identical tests carried out with pure refrigerant. Others [9, 35] have found no such increase. Kedzierski and Kaul [36], for internal flow boiling in a smooth tube, postulated that the increase in heat transfer was due to an increase in bubble site density with low viscosity oil. Increasing oil viscosity reduced the improvement in heat transfer due to offsetting effects of increased bubble site density and reduced bubble diameter. Stephan [37] attributed the increase to foaming that occurs with such mixtures. For further oil addition ($> 3\%$), the heat-transfer coefficient for these tubes has been found to decrease. It is possible that some of the above-mentioned discrepancies can be explained by the wide variety of refrigeration oils used, providing large differences in mixture properties and even varying levels of miscibility within the refrigerant. For re-entrant cavity tubes, drop-off in performance has been reported for all oil concentrations and heat fluxes [26, 27, 31, 32, 35]. This drop-off can become particularly significant for porous tubes at high oil concentrations (up to 10%) and high heat fluxes (100

kW m^{-2}). Wanniarachchi *et al.* [26] attribute this to clogging of the pores with the less volatile oil. A summary of the effects of oil on pool boiling of refrigerants from smooth and enhanced surfaces is given by Schlager *et al.* [38].

The objective of this paper is to provide a comprehensive pool boiling database for R-114 and R-114-oil mixtures from a wide variety of commercially available enhanced single tubes. A companion paper [39] extends this single tube work to smooth and enhanced tube bundles. It is appreciated that R-114 is a CFC and is to be completely phased out over the next few years due to environmental concerns over the Earth’s protective ozone layer. However, by having such a database available, the heat-transfer performance of future alternative refrigerants for flooded evaporators can be more readily evaluated. Indeed, Memory *et al.* [40] have already presented pool boiling data for R-124, a prospective replacement for R-114.

EXPERIMENTAL APPARATUS

Wanniarachchi *et al.* [26] provide complete details of the apparatus shown in Fig. 2. Two Pyrex glass tees (inside diameter 101.6 mm, length 355.6 mm) were used as the evaporator and condenser, arranged to provide reflux operation. The lower tee (evaporator) contained R-114 and the instrumented boiling tube. R-114 vapor condensed in the upper tee on a cooled copper coil and the condensate returned to the evaporator by gravity. A flow guide in the lower part of the evaporator liquid pool ensured that the returning condensate (with some associated vapor) did not interfere directly with the fluid dynamics of the boiling tube. The condenser was cooled by a refrigerated mixture of water and ethylene glycol. Pressure within the apparatus was controlled by varying the rate at which this refrigerated mixture was passed through the condenser.

Each evaporator tube (Fig. 3) had a nominal outside diameter of 15.9 mm and a total length of 450 mm. A central 190 mm portion of the tube was heated by means of a 1 kW, 240 V stainless-steel cartridge heater,‡ 6.35 mm outer diameter. To smooth out any non-uniformity in heat flux caused by the cartridge heater and to provide a convenient method to install the wall thermocouples, a copper sleeve was used inside the test tube into which the cartridge heater was inserted with a tight mechanical fit. Eight thermocouples were installed in the wall of this copper sleeve, providing temperature measurements at four circumferential and five axial positions. The copper sleeve was then carefully inserted into the evaporator test tube and carefully soldered in place to minimize any thermal contact resistance. In measuring boiling heat-transfer coefficients, great care must be exercised with the cartridge heater and temperature measuring instrumentation to ensure good accuracy. Various installation techniques have been reviewed by Jung and Bergles [33], who concluded that the heat-transfer

† All subsequent discussion uses root diameter for the low integral-fin tubes unless specifically stated otherwise.

‡ The heaters used were Watlow Firerod heaters which were continuously wound with a 203 mm nominal length and a 190 mm actual heated length.

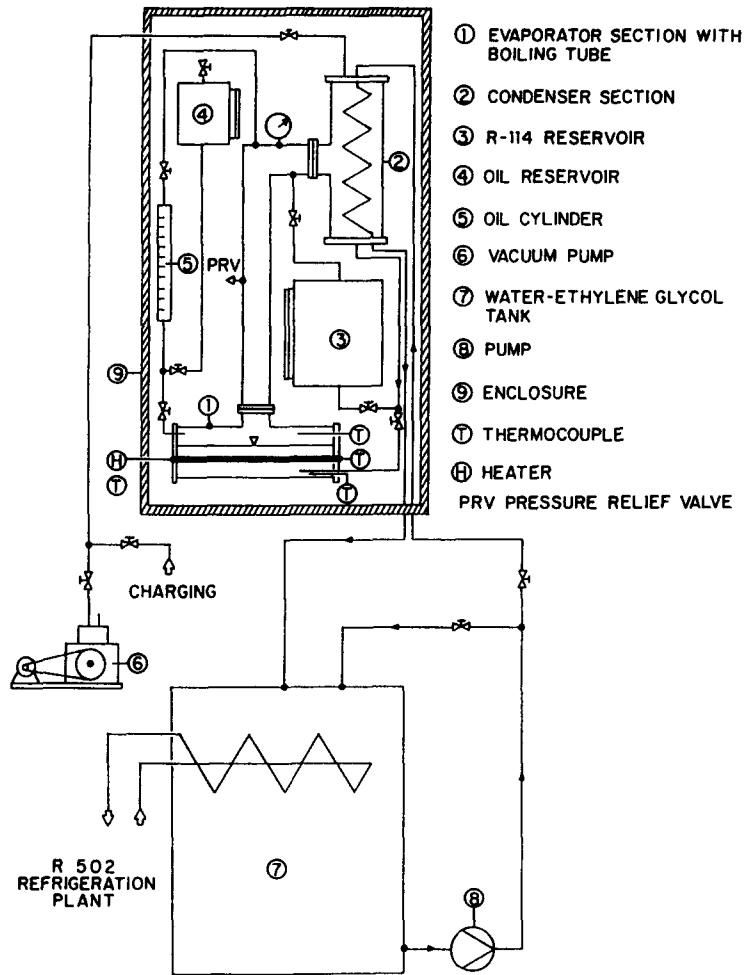


Fig. 2. Schematic of apparatus.

coefficient of a single tube in pool boiling is not sensitive to variations in the cartridge heater heat flux provided that enough thermocouples (at least four) are used to measure an average wall temperature.

Each tube was positioned accurately inside the evaporator tee by means of Teflon bushings and sealed using O-rings. These bushings fitted into aluminum end-plates at either end of the tee, again sealed using O-rings. The liquid saturation temperature in the evaporator was measured by two thermocouples placed in copper-tipped stainless-steel thermocouple wells located 8 cm from each end-plate at the same height as the evaporator tube. Another thermocouple was used to measure the vapor temperature, positioned midway along the evaporator tee, about 25 mm above the pure quiescent R-114 liquid surface. Prior to installation, all the thermocouples were carefully calibrated against a platinum resistance thermometer, giving an estimated uncertainty in the temperature measurements of ± 0.06 K. As discussed by Wanniarachchi *et al.* [26], the average liquid temperature was taken to represent the saturation temperature in preference to the vapor temperature, since the latter was seen to exceed the saturation temperature

($\approx 2.2^\circ\text{C}$) by as much as 6 K owing to radiative heat transfer from the room. A completely miscible mineral oil (York-C) was added to the evaporator via a graduated glass cylinder with a 0.5 ml resolution: Table 1 lists certain characteristics of this oil. The desired mass of oil was calculated from the initial volume of R-114 contained within the evaporator.

TUBES TESTED

The specifications of the smooth and enhanced tubes are given in Table 2. All the tubes were made of copper except the porous coated tube which had a porous copper coating on a copper-nickel base. The smooth tube was used as received with no polishing. The 19 and 26 fpi low-integral fin tubes are commercially available tubes with fin profiles that are essentially trapezoidal [GEWA-K, Fig. 1(a)], T-shaped [GEWA-T, Fig. 1(a)] and Y-shaped with notches at the base of the interfin channels [GEWA-YX, Fig. 1(b)]. The T- and Y-shaped fins are fabricated from a trapezoidal finned tube (GEWA-K) which is then rolled to provide the desired fin shape. Both of the structured surface tubes are also fabricated

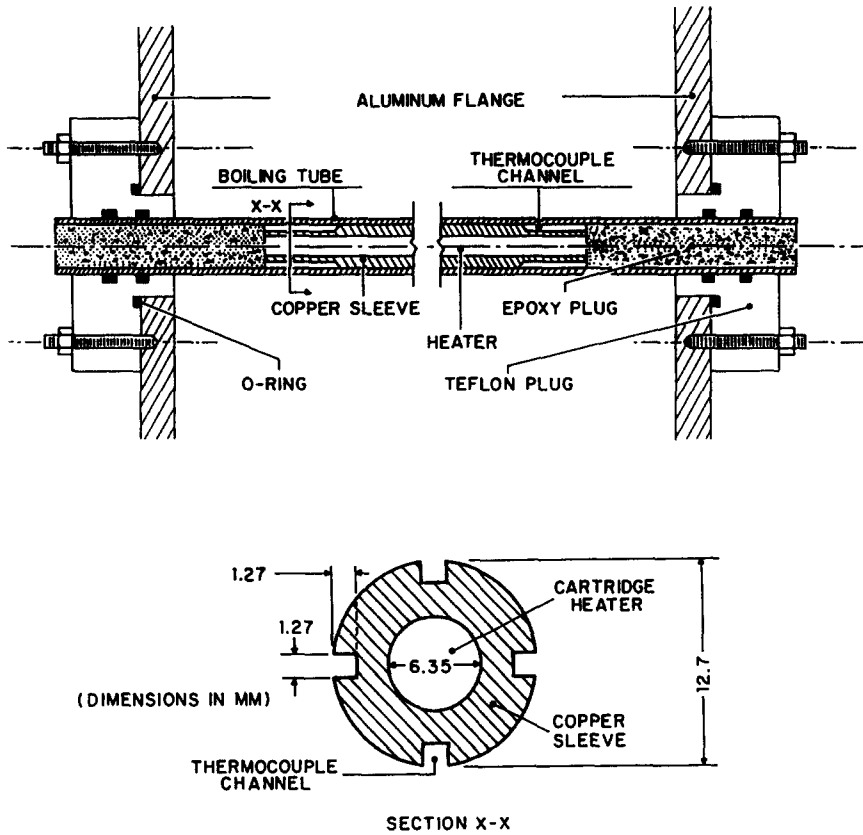


Fig. 3. Schematic of evaporator test tube.

Table 1. Characteristics of mineral oil used

Oil type	Mineral
Specific gravity @ 15.6°C	0.916
Viscosity/(cSt) @ -20°C	20 000
Viscosity/(cSt) @ 40°C	62.5
Viscosity/(cSt) @ 100°C	6.04
Pour point [°C]	-35
Flash point [°C]	180
Surface tension [N m ⁻¹]	0.045

from trapezoidal finned tubes. The TURBO-B tube [Fig. 1(c)] is then cross-grooved and rolled to provide a grid of rectangular flattened blocks that are wider than the original fins. The tubes are supplied in a variety of nominal diameters and (depending on the rolling process) size of flattened blocks (referred to as TURBO-B S, M and L), thus providing differing gap widths to suit a particular application: the present tubes used were TURBO-B M. The THERMO-EXCEL-HE tube [Fig. 1(d)] is also cross-grooved to provide triangular 'teeth' which are then rolled over to one side forming numerous triangular-shaped cavity openings. The porous tube [HIGH FLUX, Fig. 1(e)] is fabricated by spraying a smooth tube with a coating of binder, metallic powder and brazing powder. The tube is then heated to melt the brazing powder, which leaves a thin porous matrix of interconnected pass-

ageways. Particle size and coating thickness can be varied to suit a particular application. Thome [13] describes the fabrication of all these tubes in more detail.

EXPERIMENTAL PROCEDURE

Once the evaporator tube was installed, the system was evacuated to an absolute pressure of about 3 kPa. With no leaks detected over a 24 h period, the evaporator was charged with pure R-114 from a liquid reservoir (not shown in Fig. 2) to a level of 20 mm above the top of the tube. Oil concentrations of 0% (i.e. pure refrigerant), 3% and 10% were used. With 10% oil added to the system, the mixture level increased to a maximum of 32 mm above the top of the tube. For each tube, the average outer wall temperature was obtained by averaging the eight wall thermocouples in the copper sleeve and correcting for the small radial temperature drop due to conduction across the copper wall. The temperature drop across the solder joint between the copper sleeve and the test tube (estimated to be 0.05 mm thick) was neglected. For a given tube, the heat flux was calculated by dividing the electrical power (after it was corrected for small axial losses from each end of the test tube) by the tube surface area based on an active heated length of 190 mm and a diameter to the base of the enhancement (listed in Table 2).

Table 2. Specifications of tubes tested

Tube description	Diameter to base of enhancement [mm]	Thickness of enhancement or fin height [mm]	Surface area ratio†	Other characteristics
Smooth	15.9	—	—	Used as received
Finned (GEWA-K 19 fpi)	12.9	1.50	2.96	Centerline fin pitch of 1.34 mm
Finned (GEWA-K 26 fpi)	12.9	1.50	3.95	Centerline fin pitch of 0.98 mm
Modified finned (GEWA-T 19 fpi)	14.0	0.95	2.96	Centerline fin pitch of 1.35 mm; surface gap between fins of 0.25 mm
Modified finned (GEWA-T 26 fpi)	14.0	0.95	3.87	Centerline fin pitch of 0.98 mm; surface gap between fins of 0.31 mm
Modified finned (GEWA-YX 26 fpi)	13.8	1.05	3.92	Centerline fin pitch of 0.98 mm; surface gap between fins of 0.28 mm
Structured (THERMOEXCEL-HE)	15.5	0.20	‡	Average cavity mouth diameter of 0.1 mm
Structured (TURBO-B)	14.2	0.85	‡	Nominal gap width of 0.1 mm
Porous (HIGH FLUX)	15.7	0.1	‡	≈ 50% of the copper particles were < 44 μm

† Surface area ratio is defined as the actual wetted surface area divided by that for the same tube calculated using the diameter to base of enhancement.

‡ Due to the complexity of this enhanced surface, the actual wetted surface area is unknown.

During this investigation, each tube heat flux was first set at a maximum ($\approx 100 \text{ kW m}^{-2}$) for approx. 30 min, such that any non-condensables could collect in the condenser and be vented off. The apparatus was then secured and the test tube was left to stand overnight in the pool of R-114, reaching room temperature. The following morning, the tube heat flux was again set at maximum for another 10 min. Data collection then commenced with decreasing heat flux in pre-determined steps down to around 1 kW m^{-2} . Once the required heat flux in the evaporator had been fixed, the coolant flow through the condenser was adjusted to maintain the required saturation temperature in the pool at 2.2°C , corresponding to a pressure of approx. 1 atm.† All the data were obtained and reduced with a computer controlled data acquisition system: the thermophysical properties for R-114 were taken from REFPROP [41].

RESULTS AND DISCUSSION

One general observation that should be mentioned prior to discussion of the results was the oscillation that occurred in the pool for all tubes at heat fluxes higher than about 20 kW m^{-2} . This could clearly be seen as a periodic 'sloshing' of the fluid from side-to-side within the evaporator. The frequency‡ was found to be very repeatable at around 1 Hz and surprisingly independent of heat flux and oil concentration. It was thought that this might be due to the particular

geometry of the apparatus, but similar frequencies were also found in the bundle apparatus [46]. It may be that liquid circulation up over the tube leads to some kind of vortex shedding instability.

Uncertainty in the measured data

Throughout the investigation, the measured axial wall temperatures were found to vary slightly. These variations differed for each tube and appeared to be random and independent of thermocouple orientation. Consequently, they were probably caused by the tube soldering process rather than non-uniformity in the cartridge heater coils. At each heat flux, the values of the eight wall thermocouples were compared to examine the magnitude of these variations. To determine the effect that this variation had on the average heat-transfer coefficient, the wall temperature was averaged in two ways: (1) by averaging all eight thermocouples; and (2) by discarding the highest and lowest values and averaging the rest. The calculated average heat-transfer coefficient obtained from the two methods never differed by more than 6% for any of the tubes. As a consequence, the average outer wall temperature was taken to be the average of all eight thermocouples, with a correction to account for the depth of burial.

The uncertainty in the experimental data was estimated using a propagation of error analysis. The uncertainty in the wall superheat was dominated by the uncertainty in the average wall temperature. The uncertainty in the saturation temperature was estimated to be 0.1°C . The estimated uncertainty in the wall superheat varied slightly for each tube but was most significant for the re-entrant cavity tubes,

† This is a typical operating pressure in a centrifugal flooded evaporator using R-114.

‡ One cycle is taken to be a side-to-side motion of the pool surface back to its starting position.

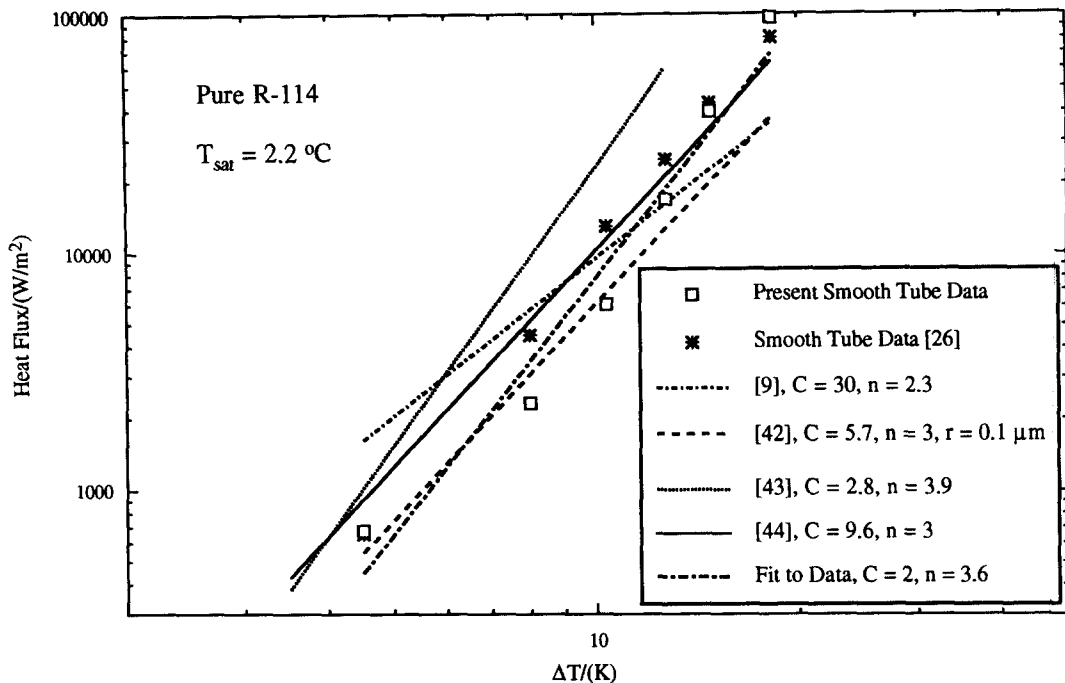


Fig. 4. Comparison of smooth tube performance for pure refrigerant with available correlations.

especially at low heat fluxes where the uncertainty is of the order of the measured wall superheat. For example, the estimated uncertainty in ΔT for the porous tube was $\pm 0.4^\circ\text{C}$ (11.4%) at high heat fluxes ($\approx 80 \text{ kW m}^{-2}$) and $\pm 0.1^\circ\text{C}$ (45%) at low heat fluxes ($\approx 2 \text{ kW m}^{-2}$). For the heat flux, the power input to the tube was measured from voltage and current sensors, estimated to be accurate to within $\pm 1\%$. The corresponding uncertainty in the measured heat flux was estimated to be 5% at low heat flux decreasing to 1.5% at high heat flux. Uncertainty bands for ΔT and the average heat-transfer coefficient for the 19 fpi trapezoidal finned and porous tubes with pure refrigerant are indicated in the figures below. Uncertainty bands for the smooth tube are too small to be included in the figures.

Smooth tube results for pure R-114

Figure 4 shows the data taken for the smooth tube with pure refrigerant. The data were very repeatable and agree closely with those of Wanniarachchi *et al.* [27], also shown. There are a number of correlations available in the literature to predict the pool boiling heat-transfer coefficient for a smooth tube in a pure liquid. Most of these can be reduced to a common form expressing heat flux as a function of wall superheat:

$$\dot{q}'' = C\Delta T^n \quad (1)$$

† It should be noted that, since equation (1) is not dimensionless, the empirical constant C has units.

‡ The value of $1 \mu\text{m}$ used here (which is not too unreasonable [43]) seems to give the best fit to the data.

where C and n are empirical constants† which typically depend on the operating pressure, thermophysical properties of the refrigerant, surface roughness and geometry of the tube. Chongrungreong and Sauer [9] developed a general correlation in terms of fluid physical properties and tube geometry. Cooper [42] included the effect of rms surface roughness (r in μm). Stephan and Abdelsalam [43] developed correlations for a wide variety of fluids by applying regression analysis to a large amount of existing data. Cornwell and Houston [44] developed a convection-based correlation, using the tube diameter as the length dimension. Using a value of surface roughness of $0.1 \mu\text{m}$ in the Cooper [42] correlation,‡ the values for C and n for all these correlations (calculated for R-114 at one atmosphere) are given in Fig. 4. Values for C and n for the present data when fitted to equation (1) are also given.

Reasonable agreement is obtained between the correlations and the present pure R-114 data, although the log-log nature of the plot can be deceiving. In particular, the correlations of Cooper [42] and Cornwell and Houston [44] do well in predicting the general trend of the data (both are within $\pm 30\%$ for the whole range of heat flux). Webb and Pais [19] also found good agreement between their data for five different refrigerants and the correlation of Cooper [42] using a value of $r = 0.3 \mu\text{m}$. This suggests that the reduced pressure, used in both correlations, is very useful as a correlating parameter. However, since the correlation of Cooper [42] is sensitive to r (which can be varied to 'fit' the data), that of Cornwell and Houston [44] is preferred.

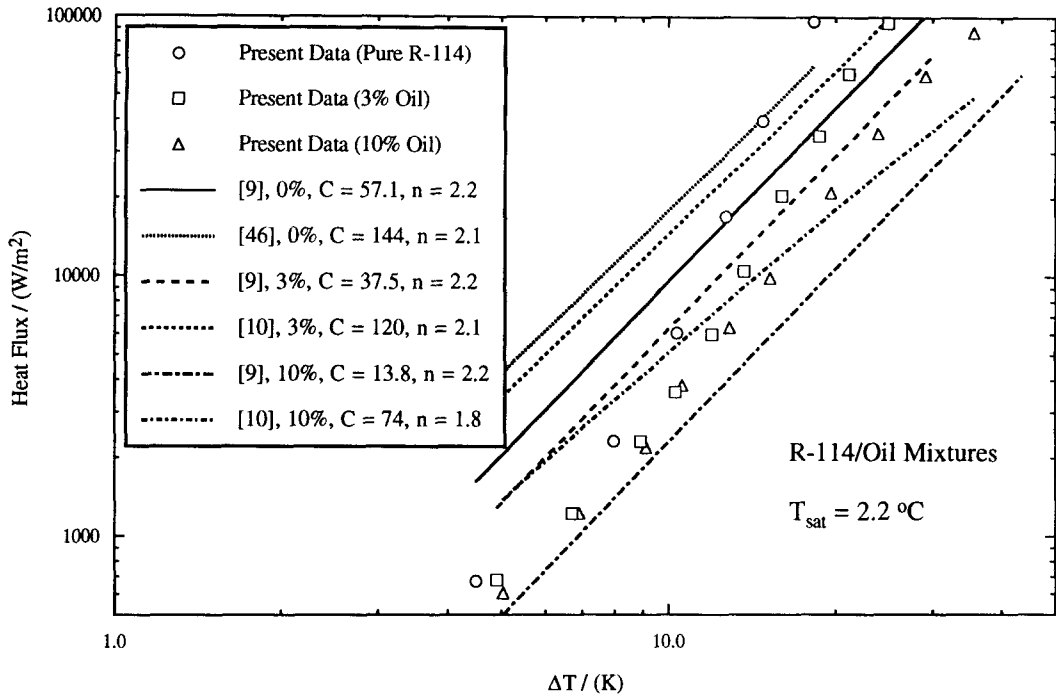


Fig. 5. Comparison of smooth tube performance for refrigerant–oil mixtures with available correlations.

Smooth tube results for R-114–oil mixtures

Figure 5 shows the smooth tube data for oil concentrations of 0, 3 and 10%. At high heat fluxes, there is a steady drop-off in performance with increase in oil concentration. At low heat fluxes, as the nucleation sites die out, the effect of the oil becomes less evident. As oil is added to a refrigerant, a number of mechanisms come into play that both increase and decrease the boiling heat transfer compared to pure refrigerant. As the more volatile refrigerant is evaporated, there is an accumulation of oil that takes place in the vicinity of the tube surface. Diffusion of oil back to the bulk mixture establishes an equilibrium concentration gradient, dependent on both bulk oil concentration and heat flux. As heat flux is increased, the boiling becomes more vigorous, and oil is transported to the surface at a faster rate, establishing a steeper concentration gradient and larger diffusion layer thickness than at low heat fluxes.

Jensen and Jackman [10] comment that steeper concentration gradients inhibit bubble growth and should lead to a drop-off in thermal performance compared to pure refrigerant. This could explain the large drop-off in thermal performance (compared to pure refrigerant) seen in Fig. 5 at high heat fluxes. At low heat fluxes, the concentration gradient is shallower and drop-off is less evident. Furthermore, as one moves from bulk fluid to the wall, the bubble point temperature increases along the concentration gradient. For a constant bulk saturation temperature, the wall temperature is then higher than that for pure refrigerant. To satisfy the constant heat flux boundary condition imposed by the electrically heated tube, the average heat-transfer coefficient then decreases with

increase in concentration gradient (increase in heat flux). Kedzierski *et al.* [45] concluded that, for binary refrigerant mixtures with widely differing boiling points, concentration gradients appeared to be the major cause of thermal degradation: this could equally apply to refrigerant–oil mixtures where the difference in boiling points is accentuated.

Unlike pure liquids, predictive methods for refrigerant–oil mixtures are very limited [9–11]. Unfortunately, all are empirically based and some require ‘fine tuning’ of constants to particular refrigerant–oil mixtures. Based on experimental data for four different refrigerant–oil mixtures, Hahne and Noworyta [11] developed an empirical correlation of the form given by equation (1). Expressions for C and n were given in terms of oil concentration and three empirical constants tuned to particular refrigerant–oil combinations. This limits its general applicability and prevents comparison with the present data.

Using R-11–oil data, Chongrungsong and Sauer [9] developed a correlation in terms of tube geometry, volume fraction of the oil (ϕ_f) and bulk mixture properties. Since property data of refrigerant–oil mixtures were limited, they also developed a much simpler relation for heat flux in terms of wall superheat, saturation pressure and ϕ_f . Surprisingly, they found that their simpler correlation did a better job of predicting heat transfer performance at higher oil concentrations. Jensen and Jackman [10] attempted to improve the modeling of refrigerant–oil mixtures by considering the accumulation of oil that takes place at the vapor bubble surface as the more volatile refrigerant is evaporated. Diffusion of this oil back to the bulk mixture establishes an equilibrium con-

centration gradient next to the bubble (or tube surface). They developed expressions for an 'effective' oil concentration (higher than the bulk concentration) in the vicinity of the growing bubble in terms of the mixture properties, mole fraction and mass diffusivity of the oil in the refrigerant, diffusion layer thickness[†] and wall superheat. These expressions were then correlated with the ratio of the experimental mixture heat-transfer coefficient (using R-113-oil and R-11-oil data) to that of pure refrigerant using a correlation of Forster and Zuber [46].

By reducing the correlations of refs. [9, 10] to the form of equation (1), they are compared with the present smooth tube data in Fig. 5: values of C and n calculated for R-114 at 1 atm are also given in the figure for pure refrigerant ($\phi_r = 1.0$) and oil concentrations of 3% ($\phi_r = 0.95$) and 10% ($\phi_r = 0.84$). It is clear that, as oil concentration increases, the slope of the data decreases. While the correlations do show a steady drop-off in thermal performance as oil concentration increases, only the model of Jensen and Jackman [10] has a decreasing slope, suggesting that it may account most accurately for the physical phenomena occurring in such mixtures. The relatively simplistic approaches used to 'model' refrigerant-oil mixtures to date demonstrate the complex nature of predicting mixture heat transfer coefficients. If mixture properties can be accurately determined (as discussed in ref. [12]) and additional mixture data provided for a variety of refrigerants, then some type of phenomenological approach could prove successful in providing more accurate physically-based models in the future.

Finned tube results for pure R-114

Figures 6 and 7 show the data for the 19 fpi trapezoidal and modified low integral-fin tubes, respectively, for 0, 3 and 10% oil concentrations. The smooth tube data are given on each figure for comparison. In general, the modified fin profile performs better than the trapezoidal fin profile under all conditions, increasing the heat transfer by between 50% and 70%. The small increase in surface area of these tubes compared to the trapezoidal finned tube ($\approx 6\%$) does not account for this increase. It is more likely to be due to the reduced spacing between fin tips creating significant differences in bubble and liquid behavior in the interfin regions. The channels created by the 'T' shaped fins tend to 'trap' bubbles such that they are forced to slide around the channel in close contact with the tube [23]. This provides a thin-liquid micro-layer between the tube and the bubble over a larger proportion of the tubes' surface, creating large heat-

transfer coefficients [47]. This trapping mechanism and improved bubble dynamics within the channels (bubble pumping) may also help to explain the apparent critical gap width dimension.

Finned tube results for R-114-oil mixtures

With 3% oil at high heat fluxes, Figs. 6 and 7 show an increase in the heat transfer (similar to that reported by other investigators). Further addition of oil (up to 10%) leads to a decrease in heat transfer. For lower heat fluxes, no such increase is observed at any oil concentration. Similar trends to those mentioned above were also found for the three 26 fpi tube profiles.[‡] The 'Y' shaped fin profile with notching in the channel base did not seem to provide any significant improvement over the 'T' shaped profile, indicating that the notches, being relatively large, provided few extra nucleation sites.

From earlier discussion on concentration gradients, addition of oil should always decrease the heat-transfer coefficient. The present finned tube data (and other reported smooth and finned tube data) contradict this and show an increase in the heat-transfer coefficient of up to 20% at low oil concentrations ($< 3\%$) and high heat fluxes. It is evident, therefore, that there must be some other mechanism that induces this increase in the presence of oil. Here, the increase is attributed to the extensive foaming that occurred when oil was added to the refrigerant.

Udomboresuwan and Mesler [48] reported significant enhancement in pool boiling heat transfer in the presence of foam. They postulated that the foam drew the liquid-vapor interface closer to the heated surface. This can have two possible enhancing effects: (1) by creating a thin liquid film between the foam and heated surface, yielding very large heat-transfer coefficients (similar to the idea of an evaporating microlayer); and (2) by bubbles leaving the surface, bursting into the neighboring liquid-vapor region (foam) and causing secondary nucleation.[§] Udomboresuwan and Mesler [48] also observed that foaming increased with heat flux, an observation also noted in the present experiments. At high heat fluxes and low oil concentrations, the enhancing effect of the foam could overwhelm the degrading effect of the concentration gradient. With increasing oil concentration, however, the gradient steepens to such an extent that it overwhelms the enhancing effect of the foam and leads to the drop-off in performance mentioned above. At low heat fluxes where there is less foaming, no such improvement is seen. Other possible explanations that may counteract the effect of the oil include some form of micro-convection occurring within the interfin region, causing better circulation and mixing close to the surface and effectively 'scouring' the oil: however, it is not likely that this would lead to an increase in heat transfer.

Table 3 gives the heat transfer enhancements at five heat fluxes for each tube at all three oil concentrations. Estimated uncertainties for the 19 fpi trapezoidal fin

[†] The diffusion layer thickness is taken to be the thickness of the oil-enriched layer.

[‡] The data for the three 26 fpi tubes are not shown in detail here, but can be gleaned from Table 3 and Fig. 10.

[§] Secondary nucleation is the entrainment of microscopic sized bubbles into superheated liquid by liquid drops penetrating a vapor-liquid interface [48].

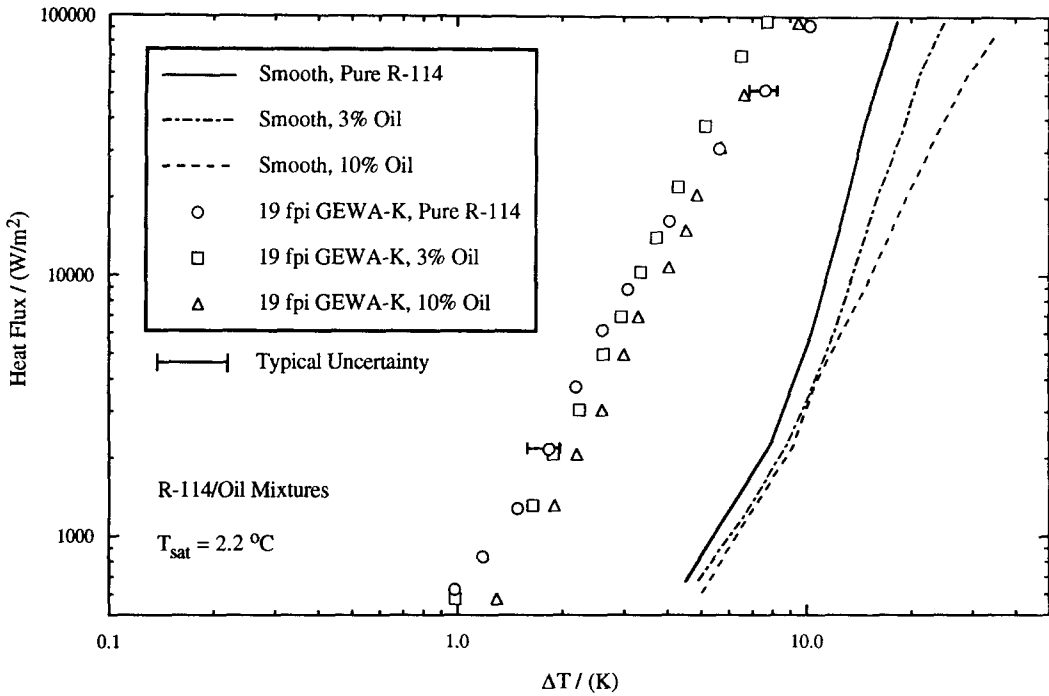


Fig. 6. Comparison of 19 fpi GEWA-K tube to smooth tube for pure refrigerant and refrigerant-oil mixtures.

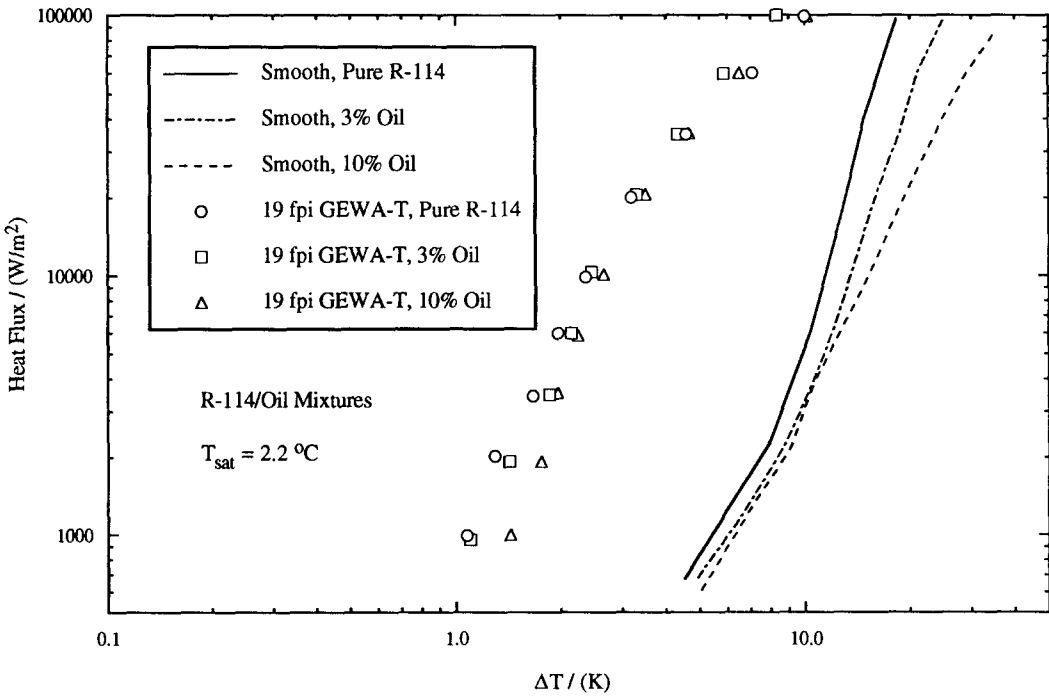


Fig. 7. Comparison of 19 fpi GEWA-T tube to smooth tube for pure refrigerant and refrigerant-oil mixtures.

tube with pure refrigerant are 15% at low heat fluxes, dropping to around 10% at high heat fluxes. Some interesting trends are seen for the finned tubes. At low heat fluxes, the effect of oil is generally small and does not affect performance too much. As heat flux increases, addition of oil significantly improves the

enhancement. At low oil concentrations, most of this improvement is due to the increases in heat transfer seen in Figs. 6 and 7. The remainder (especially at high oil concentrations) indicates that the thermal performance of the smooth tube drops off at a faster rate than the finned tubes in the presence of oil.

Table 3. Enhancement ratio for enhanced tubes

Heat flux [kW m^{-2}]	5			15			30			50			80		
Oil concentration [%]	0	3	10	0	3	10	0	3	10	0	3	10	0	3	10
Finned—GEWA-K (19 fpi)	4.0	4.4	4.0	3.1	4.0	4.1	2.5	3.7	4.1	2.1	3.6	4.1	1.8	3.3	3.9
Finned—GEWA-K (26 fpi)	3.1	3.3	3.1	2.9	3.1	3.3	2.4	2.9	3.2	2.0	2.7	2.9	1.7	2.5	2.8
Modified finned (GEWA-T 19 fpi)	5.4	5.6	5.5	4.5	5.1	5.6	3.4	4.5	5.2	2.5	3.8	4.7	2.0	3.3	3.9
Modified finned (GEWA-T 26 fpi)	5.2	4.8	4.1	4.6	4.8	4.7	3.8	4.7	4.8	3.1	4.2	4.7	2.4	3.7	4.2
Modified finned (GEWA-YX 26 fpi)	4.8	4.7	3.8	4.6	4.4	4.3	4.0	4.3	4.4	3.3	4.1	4.3	2.6	3.6	3.9
Structured (TE-HE)	>20	10.6	10.3	10.5	7.7	7.8	6.4	5.8	5.6	4.1	4.5	4.0	2.8	3.3	2.8
Structured (TURBO-B)	>20	14.7	13.7	13.1	10.7	9.3	7.0	7.5	6.3	4.4	5.0	4.4	3.3	3.6	3.3
Porous (HIGH FLUX)	18.0	13.9	13.2	10.2	9.7	9.9	7.5	6.8	4.6	5.2	4.8	2.3	3.6	3.4	1.2

Enhancement values must always be used with care as they rely heavily on the accuracy of the smooth tube data used. In addition, any comparisons between these enhancement values and those found in the literature should be made with great caution due to varying definitions of tube outer surface area. For a given heat flux, the enhancements in Table 3 are calculated from:

$$\text{enhancement} = \frac{\bar{h}_{\text{en}}}{\bar{h}_{\text{sm}}} = \frac{\dot{q}_{\text{en}}'' \Delta T_{\text{sm}}}{\dot{q}_{\text{sm}}'' \Delta T_{\text{en}}} = \frac{d_{\text{sm}} \Delta T_{\text{sm}}}{d_{\text{en}} \Delta T_{\text{en}}} \quad (2)$$

where sm \equiv smooth and en \equiv enhanced. For the smooth tube, d_{sm} is the actual outside diameter of 15.9 mm. For all the enhanced tubes, d_{en} is the diameter to the base of the enhancement, listed in Table 2. As d_{en} varies for each enhanced tube and is not equal to d_{sm} , the enhancements presented in Table 3 have a smooth-to-enhanced tube diameter ratio associated with them. In the literature, enhanced tube data are sometimes based on an envelope area, using the diameter to the fin tip or outside of the enhancement. This is the form most quoted by tube manufacturers, since existing smooth tubes are often replaced by enhanced tubes with an equal outer diameter. Enhancements based on envelope area (15.9 mm in our case) can easily be computed from Table 3 by dividing each given enhancement by the smooth-to-enhanced tube diameter ratio, $d_{\text{sm}}/d_{\text{en}}$. For example, the 19 and 26 fpi trapezoidal fin tubes have a ratio of 1.23, whereas, for the porous tube, this ratio is 1.

Another surface area often used is the actual wetted surface area: for the 19 and 26 fpi trapezoidal fin tubes, the surface area ratio (listed in Table 2) is approx. 3 and 4, respectively. At heat fluxes greater than 30 kW m^{-2} , the enhancement data given in Table 3 for these two tubes is less than this surface area ratio, indicating that the enhancement is due to the increase in surface area. This was also reported by Sauer *et al.* [16] for a 19 fpi trapezoidal fin tube. However, whereas the surface area ratio is lower for

the 19 fpi tube, the enhancements are higher, indicating that lower fin density may be preferable. The T- and Y-shaped fin profiles have similar surface area ratios as the 19 and 26 fpi tubes. However, the enhancements are now larger, possibly due to the mechanisms mentioned earlier.

Re-entrant cavity tube results for pure R-114

Figures 8 and 9 show data for one of the structured surface tubes (TURBO-B) and the porous tube, respectively, for oil concentrations of 0, 3 and 10%. Such detailed data for the other structured surface tube (THERMOEXCEL-HE) have been omitted: however, enhancements for all three tubes are listed in Table 3 for the same heat fluxes as the finned tubes. Estimated uncertainties in the enhancements for the porous tube with pure refrigerant are 30% at low heat fluxes, dropping to around 13% at high heat fluxes. Typical uncertainty bands for ΔT have also been shown for the porous tube at low and high heat fluxes in Fig. 9. The large uncertainty at low heat fluxes is typical of re-entrant cavity tubes and indicative of the fact that the uncertainty in the measured wall superheat is of the same order of magnitude as the wall superheat itself. For pure refrigerant at low to medium heat fluxes, the enhancements are high for all three tubes, indicating that there are still a significant number of active nucleation sites at these low heat fluxes. Increased pumping action within the channels or pores (caused by capillary and/or convective forces) may also be helping to increase the enhancement by drawing in fresh liquid. At higher heat fluxes, the enhancements for the re-entrant cavity tubes (and their associated uncertainties) decrease, but are still significantly greater than both the finned and smooth tubes.

Re-entrant cavity tube results for R-114-oil mixtures

With the addition of small quantities of oil (up to 3%), the heat transfer rate decreases for all three re-

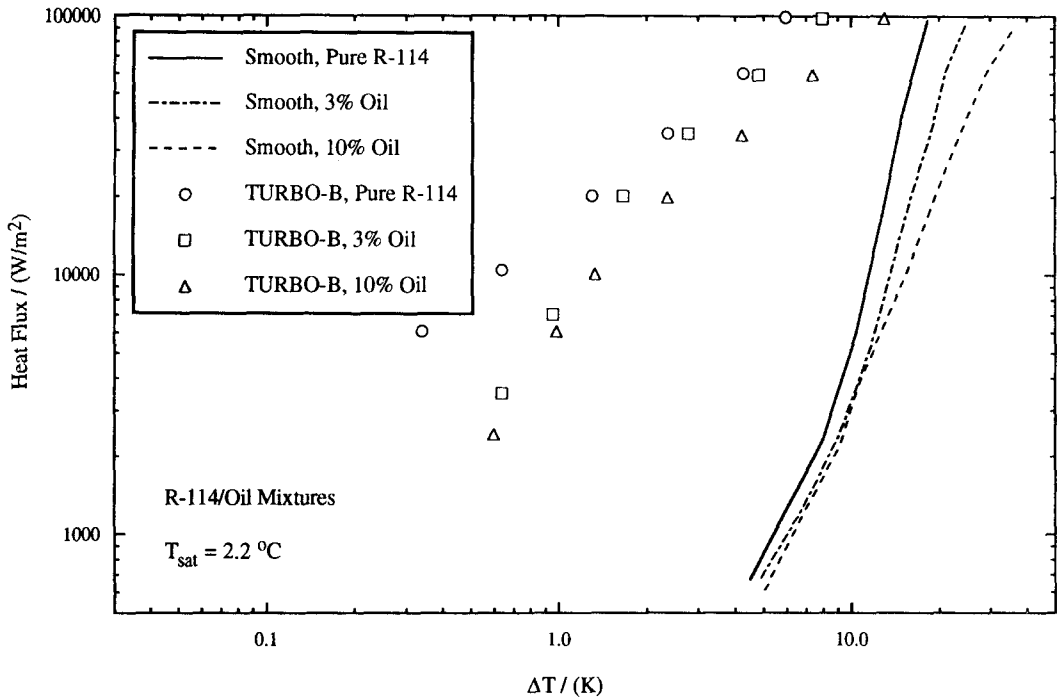


Fig. 8. Comparison of TURBO-B tube to smooth tube for pure refrigerant and refrigerant-oil mixtures.

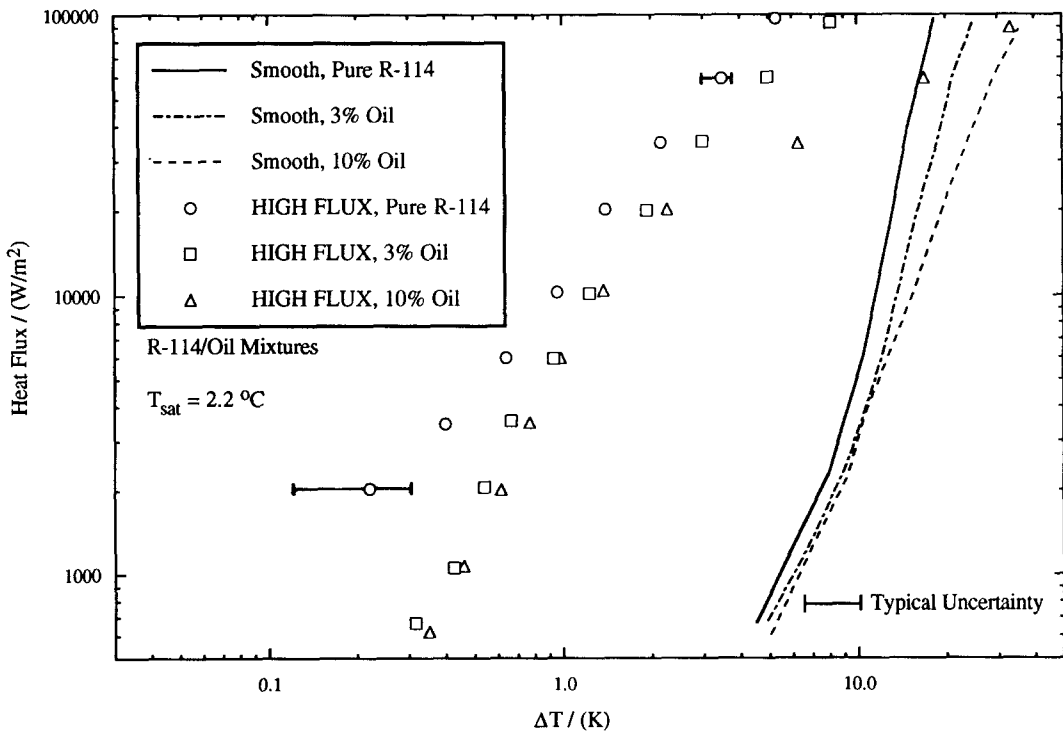


Fig. 9. Comparison of HIGH FLUX tube to smooth tube for pure refrigerant and refrigerant-oil mixtures.

entrant cavity tubes, even though foaming was still very evident. Improvement in heat transfer with small quantities of oil has never been reported for re-entrant cavity tubes. This may be for a number of reasons: (1) the foam cannot penetrate the re-entrant cavities

where the majority of the heat transfer takes place; (2) the oil, once inside the cavity, cannot easily diffuse back to the bulk mixture; and (3) a higher rate of oil is transported to the surface due to the higher density of active nucleation sites per unit area. At a given heat

flux, (2) and (3) give rise to a steeper concentration gradient than for a smooth or finned tube, perhaps overwhelming any beneficial effect of the foam.

At low oil concentrations and high heat fluxes, enhancement for the two structured surface tubes increases, again due to the thermal performance of the smooth tube dropping off at a faster rate in the presence of oil. The structured surface tubes therefore seem to display some of the characteristics of finned tubes, which is perhaps not too surprising when one considers how they are made. Such an increase is not seen for the porous tube, suggesting that the con-

trolling heat transfer mechanisms are different for each type of re-entrant cavity tube in the presence of oil. This is supported by the fact that, with further addition of oil, the thermal performance of the two structured surface tubes drops off only slightly compared with that for the porous tube, which drops off so dramatically that an enhancement of only 20% is obtained at high heat fluxes. Wanniarachchi *et al.* [26] suggested that the porous tube (which has a relatively random pore size distribution) becomes more readily 'clogged' with oil, leading to exceptionally high thermal resistances. Liquid and vapor trapped in the

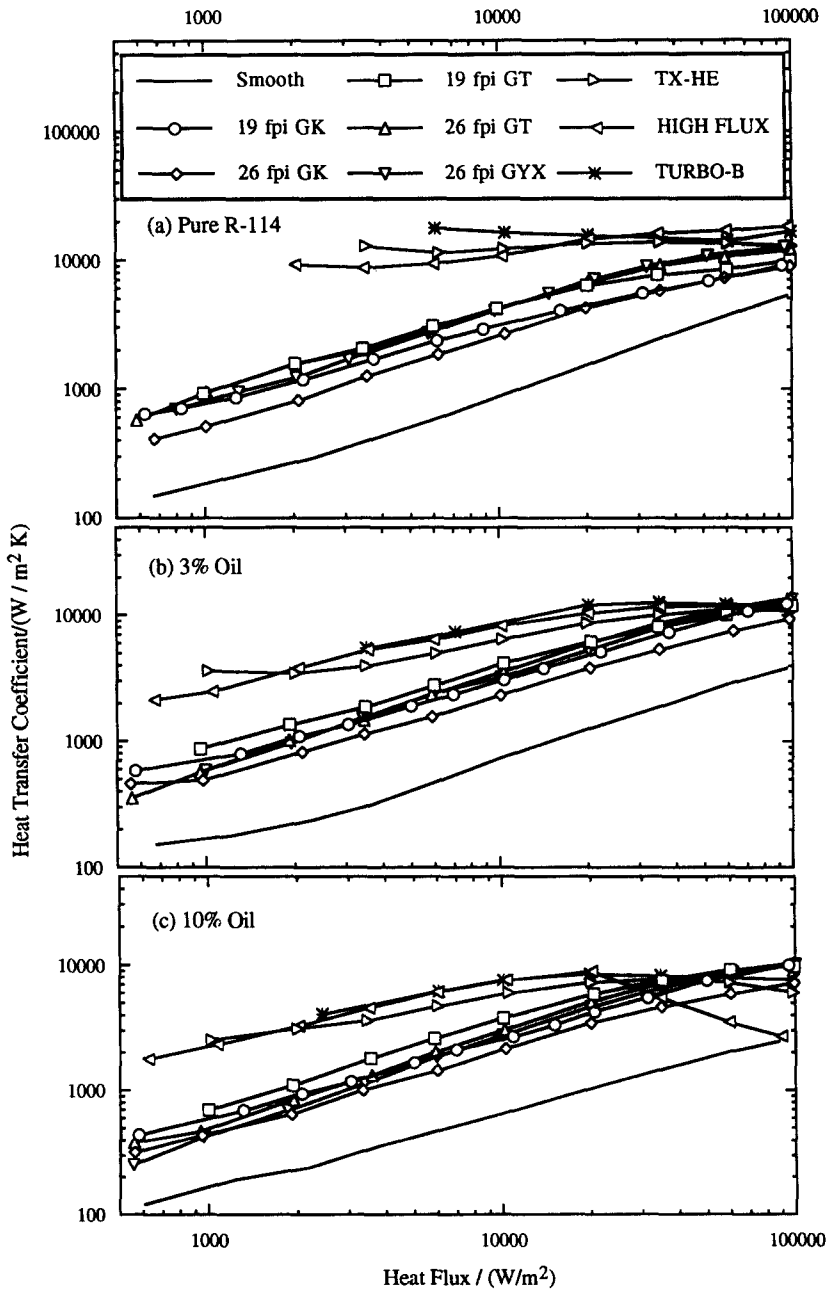


Fig. 10. Heat-transfer coefficient vs heat flux for all tubes at 0, 3 and 10% oil concentration (GK = GEWA-K, GT = GEWA-T, GYX = GEWA-YX, TX-HE = THERMOEXCEL-HE).

organized (man-made) cavities of a structured surface tube can probably move about (and diffuse) more freely than in the disorganized (random) cavities of a porous tube, giving better heat transfer and less clogging. It should be pointed out, however, that oil is detrimental for all three re-entrant cavity tubes such that, at high heat fluxes and high oil concentrations, the modified fin profile tubes provide the best overall thermal performance.

Figure 10(a)–(c) presents a summary of the data for the nine tubes for oil concentrations of 0, 3 and 10%, respectively. The data, plotted as average heat-transfer coefficient vs heat flux, clearly show three distinct 'types' of surface: (1) smooth, (2) low integral-fin (trapezoidal and modified fin profiles), and (3) re-entrant cavity. At low heat fluxes, the three groups are fairly distinct for each oil concentration. At high heat fluxes, however, the groups tend to merge, especially the latter two as oil concentration increases. At the highest heat fluxes for pure refrigerant, the advantage of using a re-entrant cavity tube is evident. As oil concentration is increased, however, the heat transfer from each re-entrant cavity tube decreases and the integral-fin tubes with modified fin profiles provide the best performance at high heat fluxes. The poor performance of the porous coated tube at high heat fluxes with 10% oil can also be clearly seen. At design heat fluxes ($15\text{--}30\text{ kW m}^{-2}$ for most commercial flooded evaporators) and oil concentrations ($<3\%$ with separators), enhancements are still significantly larger for all three of the re-entrant cavity tubes than for any of the finned tubes.

CONCLUSIONS

An experimental database has been established for pool boiling of pure R-114 and R-114–oil mixtures from single tubes having smooth and enhanced surfaces. Based on these single tube measurements, the following conclusions may be made.

Pure R-114

- For finned tubes at a given heat flux, a profiled fin shape creates a gap width which can increase heat transfer, possible due to improved bubble dynamics within the channels.
- The re-entrant cavity tubes provide the largest enhancements due to the higher density of active nucleation sites and perhaps better fluid pumping within the channels. As heat flux decreases, this improvement becomes more significant due to the increasing ratio of active sites compared to those on a finned or smooth tube.

R-114–oil mixtures

- For the finned tubes at high heat fluxes, small quantities of oil (up to 3%) increase the heat transfer coefficient: this is thought to be associated with the foaming that accompanies the boiling of such

mixtures. Further increases in oil concentration lead to a steady decrease in performance.

- For the re-entrant cavity tubes, any addition of oil leads to a drop-off in performance. This is especially significant for the porous coated tube at high heat fluxes and high oil concentrations (up to 10%), where it is thought that the oil tends to clog up the pore structure.
- The trends of the data can be explained from consideration of the various mechanisms which transport oil to and from the heated surface.
- At practical design heat fluxes ($15\text{--}30\text{ kW m}^{-2}$) and oil concentrations ($\approx 3\%$) for flooded type evaporators, the re-entrant cavity tubes provide the best thermal performance.

Acknowledgments—This work was partially supported by Mr R. Helmick, Naval Surface Weapons Center, Carderock Division, Annapolis Detachment. The authors would like to thank Mr P. Thors at Wolverine Tube Co, Mr K. Menze at Wieland-Werke AG, Dr E. Ragi at UOP and Dr W. Nakayama at Hitachi for supplying the tubes.

REFERENCES

1. W. Leiner and D. Gorenflo, Methods of predicting the boiling curve and a new equation based on thermodynamic similarity. In *Pool and External Flow Boiling* (Edited by V. Dhir and A. E. Bergles), pp. 99–103. ASME (1992).
2. V. P. Carey, *Liquid–Vapor Phase-Change Phenomena*, Chaps 6 and 7. Hemisphere, Washington, DC (1992).
3. K. Stephan, *Heat Transfer in Condensation and Boiling*, pp. 145–155. Springer, Berlin (1992). [Translated from the first German edition. Springer, Berlin (1988).]
4. E. Hahne, Q. Chen and R. Windisch, Pool boiling heat transfer on finned tubes—an experimental and theoretical study. *Int. J. Heat Mass Transfer* **34**(8), 2071–2079 (1991).
5. J. Chen, L. Dong and H. Zhang, Boiling heat transfer on low finned tube. *Advances in Phase Change Heat Transfer—Proceedings of the International Symposium on Phase Change Heat Transfer*, China, pp. 129–134 (1988).
6. K. Nishikawa and T. Ito, Augmentation of nucleate boiling heat transfer by prepared surfaces. In *Heat Transfer in Energy Problems* (Edited by T. Mizushima and W. J. Yang), pp. 111–118. Hemisphere, Washington, DC (1982).
7. M. Xin and Y. Chao, Analysis and experiment of boiling heat transfer on T-shaped finned surfaces, *23rd National Heat Transfer Conference*, Denver (1985).
8. W. Nakayama, T. Daikoku, H. Kuwahara and T. Nakajima, Dynamic model of enhanced boiling heat transfer on porous surfaces. *J. Heat Transfer* **102**, 451–456 (1980).
9. S. Chongrungrong and H. J. Sauer Jr, Nucleate boiling performance of refrigerants and refrigerant–oil mixtures. *J. Heat Transfer* **102**, 701–705 (1980).
10. M. K. Jensen and D. L. Jackman, Prediction of nucleate pool boiling heat transfer coefficients of refrigerant–oil mixtures. *J. Heat Transfer* **106**, 184–190 (1984).
11. E. Hahne and A. Noworyta, Calculation of heat transfer coefficients for nucleate boiling in binary mixtures of refrigerant–oil. *Int. Commun. Heat Mass Transfer* **11**(4), 417–429 (1984).
12. J. R. Lloyd and P. J. Marto, A predictive method to describe the boiling behavior of refrigerant–oil mixtures,

- Technical Report no. NPS69-90-07, NPS, Monterey, CA (1990).
13. J. R. Thome, *Enhanced Boiling Heat Transfer*. Hemisphere, Washington, DC (1990).
 14. R. L. Webb, *Principles of Enhanced Heat Transfer*, Chap. 11. Wiley, New York (1994).
 15. N. Arai, T. Fukushima, A. Arai, T. Nakajima, K. Fujie and Y. Nakayama, Heat transfer tubes enhancing boiling and condensation in heat exchangers of a refrigerating machine, *ASHRAE Trans.* **83**, Pt 2, 58–70 (1977).
 16. H. J. Sauer Jr, G. W. Davidson and S. Chongrungreong, Nucleate boiling of refrigerant-oil mixtures from finned tubing, *ASME/AICHE National Heat Transfer Conference*, paper no. 80-HT-111, Orlando, FL (1980).
 17. T. C. Carnavos, An experimental study: pool boiling of R-11 with augmented tubes. In *Advances in Enhanced Heat Transfer*, HTD-Vol 18, pp. 103–108. ASME, New York (1981).
 18. Z. H. Ayub and A. E. Bergles, Pool boiling from GEWA surfaces in water and R-113. In *Augmentation of Heat Transfer in Energy Systems*. HTD-52, pp. 57–66. ASME, New York (1985).
 19. R. L. Webb and C. Pais, Nucleate pool boiling data for five refrigerants on plain, integral-fin and enhanced tube geometries, *Int. J. Heat Mass Transfer* **35**(8), 1893–1904 (1992).
 20. D. Gorenflo, P. Sokol and S. Caplanis, Pool boiling heat transfer from single tubes to new refrigerants, *18th International Congress of Refrigeration*, Vol. II, pp. 423–428 (1991).
 21. P. J. Marto, A. S. Wanniarachchi and R. J. Pulido, Augmenting the nucleate pool boiling characteristics of GEWA-T finned tubes in R-113. In *Advances in Enhanced Heat Transfer*, HTD-Vol. 18, pp. 67–73. ASME, New York (1981).
 22. K. Stephan and J. Mitrovic, Heat transfer in natural convective boiling of refrigerants and refrigerant-oil mixtures in bundles of T-shaped finned tubes. In *Advances in Enhanced Heat Transfer*, HTD-Vol. 18, pp. 131–146. ASME, New York (1981).
 23. K. Stephan and J. Mitrovic, Heat transfer in natural convective boiling of refrigerant-oil mixtures, *Proceedings of the 7th International Heat Transfer Conference*, Munich, Vol. IV, pp. 73–87 (1982).
 24. P. J. Marto and V. J. Lepere, Pool boiling heat transfer from enhanced surfaces to dielectric fluids, *J. Heat Transfer* **104**, 292–299 (1982).
 25. P. J. Marto and B. Hernandez, Nucleate pool boiling characteristics of a GEWA-T surface in R-113, *AICHE Symp. Ser.* **79**(225), 1–10 (1983).
 26. A. S. Wanniarachchi, P. J. Marto and J. T. Reilly, The effect of oil contamination on the nucleate pool boiling performance of R-114 from a porous-coated surface, *ASHRAE Trans.* **92**, Pt 2, 525–538 (1986).
 27. A. S. Wanniarachchi, L. M. Sawyer and P. J. Marto, Effect of oil on pool boiling performance of R-114 from enhanced surfaces, *Proceedings of the 2nd ASME/JSME Thermal Engineering Conference*, Honolulu, Vol. 1, pp. 531–537 (1987).
 28. K. E. Starner and R. A. Cromis, Energy savings using HIGH FLUX evaporator surface in centrifugal chillers, *ASHRAE J.* **19**(12), 24–27 (1977).
 29. A. E. Bergles and M. C. Chyu, Characteristics of nucleate pool boiling from porous metallic coatings, *J. Heat Transfer* **104**, 279–285 (1982).
 30. R. Antonelli and P. S. O'Neill, Design and application considerations for heat exchangers with enhanced boiling surfaces. In *Heat Exchanger Sourcebook* (Edited by J. W. Palen), pp. 645–661. Hemisphere, Washington, DC (1986).
 31. I. Grant, G. F. Hewitt and J. Qureshi, Pool boiling of R-113-oil mixtures on a HIGH FLUX tube, *Advances in Pool Boiling Heat Transfer—Proceedings of Eurotherm 8*, Paderborn, pp. 169–172 (1989).
 32. C. Marvillet, Influence of oil on nucleate pool boiling of refrigerants R-12 and R-22 from porous layer tube, *Advances in Pool Boiling Heat Transfer—Proceedings of Eurotherm 8*, Paderborn, pp. 164–168 (1989).
 33. C. Jung and A. E. Bergles, Evaluation of commercial enhanced tubes in pool boiling, Energy Conservation Report no. DOE/ID/12772-1, RPI, Troy, NY (1989).
 34. K. I. Bell, G. F. Hewitt and S. D. Morris, Nucleate pool boiling of refrigerant/oil mixtures, *Expl Heat Transfer* **1**, 71–86 (1987).
 35. R. L. Webb and W. F. McQuade, Pool boiling of R-11 and R-123 oil-refrigerant mixtures on plain and enhanced tube geometries, *ASHRAE Trans.* **99**, Pt 1 (1993).
 36. M. A. Kedzierski and M. P. Kaul, Horizontal nucleate flow boiling heat transfer coefficient measurements and visual observations for R-12, R-134a, and R-134a/ester lubricant mixtures, *6th International Symposium on Transport Phenomena in Thermal Engineering*, Seoul, Vol. 1, pp. 111–116 (1993).
 37. K. Stephan, The effect of oil on heat transfer of boiling R-12 and R-22, *Kaeltetechnik* **16**(6), 162–166 (1964) (in German).
 38. L. M. Schlager, M. B. Pate and A. E. Bergles, A survey of refrigerant heat transfer and pressure drop emphasizing oil effects and in-tube augmentation, *ASHRAE Trans.* **9**, Pt 1, 392–416 (1987).
 39. S. B. Memory, N. Akcasayar, H. Eraydin and P. J. Marto, Nucleate pool boiling of R-114 and R-114-oil mixtures from smooth and enhanced surfaces—II. Tube bundles, *Int. J. Heat Mass Transfer* **38**, 1363–1376 (1995).
 40. S. B. Memory, G. Bertsch and P. J. Marto, Pool boiling of HCFC-124-oil mixtures from smooth and enhanced surfaces. In *Heat Transfer With Alternate Refrigerants*, HTD-Vol. 243, pp. 9–18. ASME, New York (1993).
 41. J. Gallagher, M. McLinden and G. Morrison, *REFPROP: Thermodynamic Properties of Refrigerants and Refrigerant Mixtures*. NIST, Gaithersburg, MD (1991).
 42. M. G. Cooper, Saturation nucleate pool boiling—a simple correlation, *Int. Chem. Engng Symp. Ser.* **86**, 785–792 (1984).
 43. K. Stephan and M. Abdelsalam, Heat transfer correlations for natural convection boiling, *Int. J. Heat Mass Transfer* **23**, 73–87 (1980).
 44. K. Cornwell and S. D. Houston, Nucleate pool boiling on horizontal tubes: a convection-based correlation, *Int. J. Heat Mass Transfer* **37**(Suppl. 1), 303–309 (1994).
 45. M. A. Kedzierski, J. H. Kim and D. A. Didion, Causes of the apparent heat transfer degradation for refrigerant mixtures. In *Two-phase Flow and Heat Transfer*, HTD-Vol. 197, pp. 149–158. ASME, New York (1992).
 46. H. K. Forster and N. Zuber, Dynamics of vapor bubbles and boiling heat transfer, *A.I.Ch.E. J.* **1**, 531–535 (1955).
 47. K. Cornwell, The influence of bubbly flow on boiling from a tube in a bundle, *Advances in Pool Boiling Heat Transfer—Proceedings of Eurotherm Seminar 8*, Paderborn, pp. 177–183 (1989).
 48. A. Udombaresuwan and R. Mesler, The enhancement of nucleate boiling by foam, *Proceedings of the 8th International Heat Transfer Conference*, San Francisco, Vol. 6, pp. 2939–2944 (1986).